Geosynthetics: Applications, Design and Construction, De Groot, Den Hoedt & Termaat (eds)
 ISBN 90 5410 836 3

Laboratory study and numerical analysis for pull-out behaviors of geogrids confined by weathered mudstone and sandy soil

Dave Ta-Teh Chang & Fan-Yi Hung
Civil Engineering Department, Chung Yuan University, Chung Li, Taiwan
Tsung-Sheng Sun
Joy View Enterprise Corporation, Kuang-Fu, Taiwan

ABSTRACT : Among the pull-out behaviors of geogrids, it is important to note that pull-out resistance tends to increase along with increases in confinement pressure. For semi-rigid geogrids covered by cohesiveless particulate soils, most of the pull-out resistance of the geogrid is provided by passive soil resistance, while the greater portion of the pull-out resistance for geogrids covered by cohesive particulate soils is provided by friction. Using numerical analysis to simulate the conditions of the reinforced soil slope, it was found that sand backfill materials provided excellent results, while a relatively greater amount of weathered mudstone was needed for the same amount of reinforcement. When considering the use of fine grained soil as backfill, if undrainage is present, attention must be given to the grid's anchorage strength as force is exerted on the the soil structure.

Introduction

The main function of reinforcement material is to limit the level of displacement of the soil structure. The interactive frictional effect of the grains of soil in the reinforcement structure coming in contract with the surface of the reinforcement material limits the deformation of the soil structure. Thus, reinforcement overcomes the deficiencies of the tensile strength in the soil. Geogrids provide two sources of resistance to the pull-out failure mechanism in the soil structure which are: (1) The friction in the contact plane between the soil and geogrid. (2) Passive earth resistance of the soil coming in contact with the transverse ribs. To meet economical design criteria, it is desirous that materials available on scene be used as backfill. The route of Taiwan Second National Freeway passes through a primarily mudstone area. To understand the suitability of reinforment materials, a demonstration retaining wall was constructed in Tienliau Village, Kaohsiung. Focusing on interactive pull-out behaviors for comparative discussion, this study used weathered mudstone and sandy soil as backfill material, and two types of geogrid to conduct as series of geogrid pull-out tests. At the same time the results of laboratory tests were used to establish parameters of a numerical analysis system, which could be used to analyze the suitability of the two above mentioned soils as backfill materials in reinforced structures.

Frictional resistance is produced by the interaction between the surface of the geogrid and the soil. Due to the grid-shaped construction, the transverse ribs of the geogrid interlock tightly with the intervening soil, and pull-out causes the geogrid to move in relation with the soil, producing passive resistance between the transverse ribs and the soil it surrounds [1].

Bauer [2]et al. pointed out that the effect the special properties of the soil and the geogrid had on pull-out resistance behaviors were two factors that must be considered. There are two methods for evaluating the pull-out resistance of soil/geogrid in the laboratory [3]which are: (1) The geogrid produces pull-out resistance during the pull-out test, which is a combination of the two aforementioned types. (2) The test uses the maximum pull-out force to calculate average pull-out resistance. The results of these two methods are used for design and analysis.

Contents and Methods of Experiment

Specimen Preparation

Two types of unidirectional geogrids--labeled A and B--manufactured from HDPE(detailed measurements

and related properties are listed in Table 1). To reduce the influence of the boundary effect, an 8-grid-square wide and 3-grid-square long sample of both A and B were buried at a fixed length of 39 cm. Additionally, to better understand the net frictional properties between the soil and grid, pull-out tests were performed on geogrids with the transverse ribs removed. With the effective contact area of the modified geogrid, the total surface plane of the unmodified grid along with the frictional resistance of the soil can be determined. Moreover, passive earth resistance between the transverse ribs and the soil can be compared using this method.

Of the sandy soils used in this test program, one was collected from the backfill used for the test wall in Tienliao, Kaohsiung County, and its relative density was controlled at 80 %. The fine soils used were obtained from the in-situ mudstone. Water content controlled at OMC + 2 %, and compaction was maintained at 95 %. Basic properties of these soils are listed in Table 2.

Testing Device and Experimental Procedures

This study employed a pull-out box, with internal dimensions of both top and bottom boxes measuring 40 cm long by 50 cm wide by 15 cm deep, with a 1 mm opening between the two boxes remaining to perform confined pull-out testing. Normal stress was applied by a rubber membrane. The pulling system used a fixed speed motor system which applied a stable rate of strain. An LVDT accurate to 10^{-3} mm, along with an amplifier and a 5-ton load cell attached were used to measure the amount of pull-out.

Burying the geogrid at a fixed length controlled at 39 cm, confining pressure is applied at 0.5 kg / cm^2, 1.0 kg / cm^2, and 1.5 kg / cm^2 respectively, with pulling speed set at 1 mm / min [4]. Soil is compacted into the top and bottom boxes in 5 uniform layers, with the geogrid sandwiched in the middle. The grid along with the clamps are adjusted to maintain the specimen in a level position, so that force is evenly applied. Static pressure is then supplied in the required amount to the upper membrane. When pull-out force is applied, the value is read by data logger until force values begin to decrease.

Numerical Analysis Model

This study utilized the explicit finite difference code of the Fast Lagrangian Analysis of Continua (FLAC) to establish a numerical analysis model. This model was used to simulate the pull-out behaviors of the

Table 1: Geogrid dimensional measurements and results of tension tests

Geogrid	A	B
Shape of apertures	oblong	oblong
Thickness of longitudinal ribs, mm	1.4	0.95
Length of longitudinal ribs, mm	144	144
Width of transverse ribs, mm	16	16
Thickness of transverse ribs, mm	3.9	2.7
Tensile strength, kN/m	87	60
Elongation, %	10.8	8.8
Young's Modulus, E N/m^2	9.286×10^8	1.053×10^8
Yield Strength N/m	8.7×10^4	6.0×10^4

Table 2: Soil Properties tested and parameter selection values

Property	Backfill sand	Weathered mudstone
Dry unit weight, γ (kg/m^3)	1791	1865
Angle of internal friction , f	45 °	29 °
Cohesion, C (N/m^2)	------	3.565×10^4
Shear Modulus S ($N/m^2/m$)	6×10^7	6.4×10^7
Bulk Modulus B($N/m^2/m$)	$1\times10^{8[**]}$	1.07×10^8

Note: [**] are suggested design values

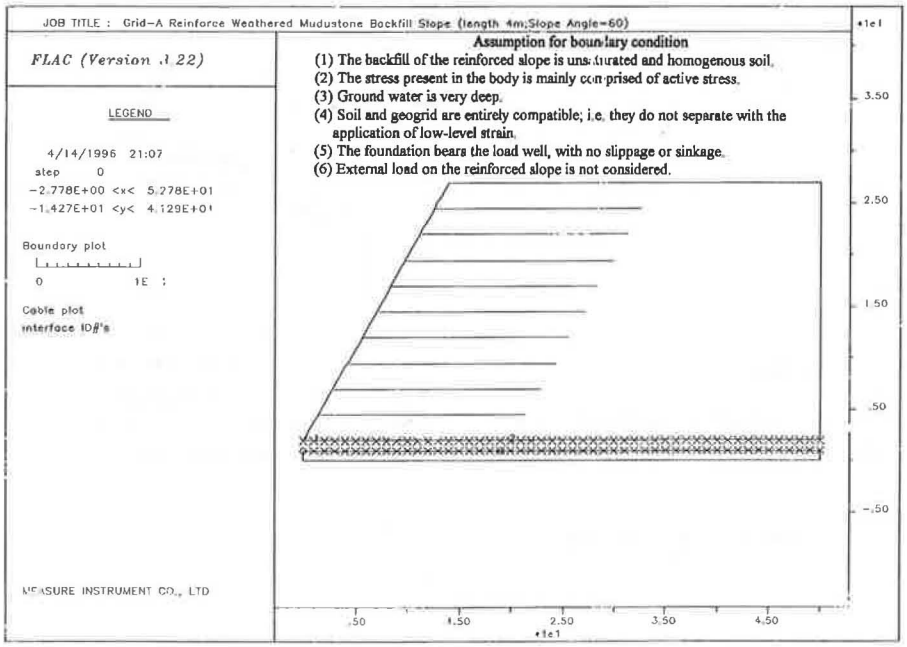

Figure 1--Numerical simulation of boundary conditions of reinforced slope.

soil specimens, and the conditions of the reinforced soil body system. In this model, cable was selected as the simulation element for the geogrid. Pulling at a fixed rate, the FISH function was used to calculate the total resistance and displacement of the cable during pull-out tests. These results were then compared with actual pull-out test results of soil/geogrid specimens.

Related soil parameters that must be entered in the FLAC program include the soil unit weight, cohesion, frictional angle, shear modulus, and bulk modulus. The initial three parameters can be directly determined from laboratory tests. The shear modulus utilizes the slope determined from the shear stress-strain chart of the direct shear test. The bulk modulus adopts the value suggested by Cundall [5], author of the FLAC program (See Table 2 for soil selection parameter values). Reinforcement element parameters include Young's modulus, yield strength, and the cross areas. The former two can be determined from tensile testing. The geogrid is assumed as uniform. (See Table 1).

When stretching the cable element to simulate the behavior of the grid, the chief parameter for the mechanical transfer between the soil and geogrid originates from the shear stiffness of grout (K_{bond}), and the slider cohesiveness of grout (S_{bond}). The parameters needed for this simulation must be similar to the interactive behaviors of the pull-out test. Therefore, this simulation utilizes the K_{bond} and S_{bond} results of the pull-out test.

A 25 m high, 60 ° gradient slope with vertical reinforcement spaced at 2.5 m intervals buried to a depth of 20 m was used to evaluate the pull-out behavior of the total body of reinforced slope (See Figure 1). The purpose of designing such a tall wall with such a steep slope is to emphasize the significance of stress-strain behaviors for reinforcement. To simplify analysis procedures, this model used some idealized conditions which are lised in Figure 1.

Moreover, S_{bond} is a function of restrain stress, with strength increasing in direct proportion to the increase in normal stress. In the numerical simulation of the pull-out test, the parameters depend on the functional relationship of differing confinement conditions. The foundation elements are assumed as the mass without sliding and settlement. The mechanical properties of stiffness and strength differ between lower-level reinforcement and the foundation elements, which could cause non-convergence between soil and geogrid. As a result, this study adds the interface to

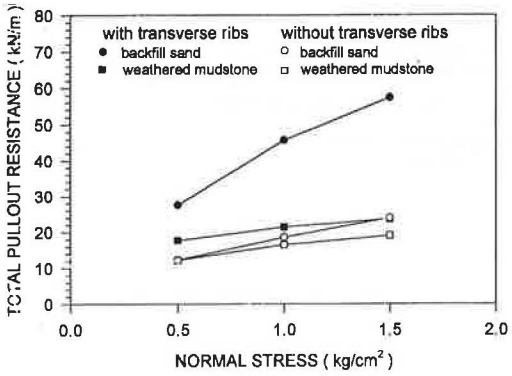

Figure 2--Comparison of pull-out resistance in grid A with and without transverse ribs

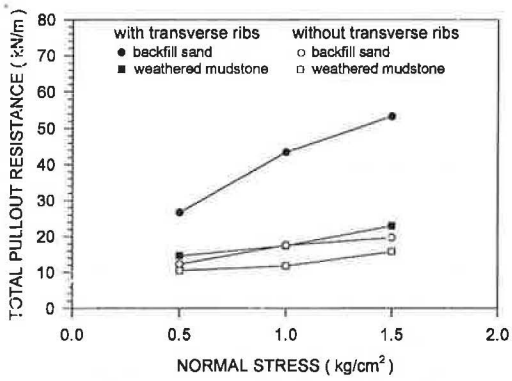

Figure 3--Comparison of pull-out resistance in grid B with and without transverse ribs

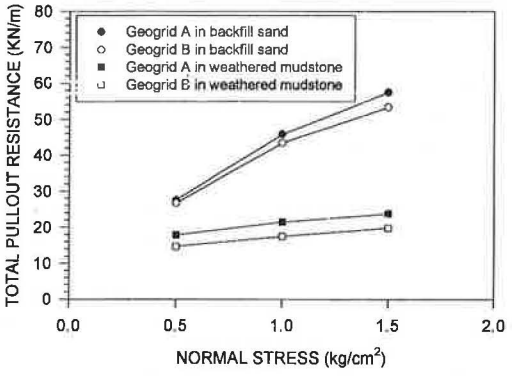

Figure 4--Total pull-out resistance between grid and soil under various confinement

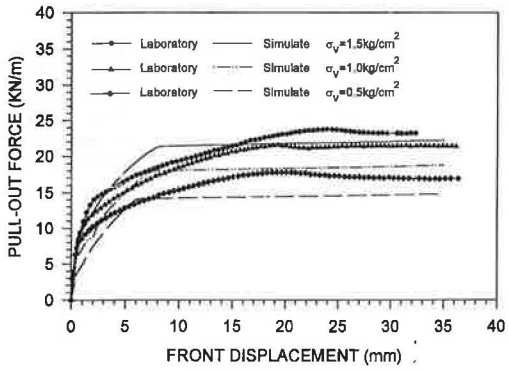

Figue 5--Pull-out force/displacement chart for laboratory test and numerical simulation of grid A confined under weathered mudstone.

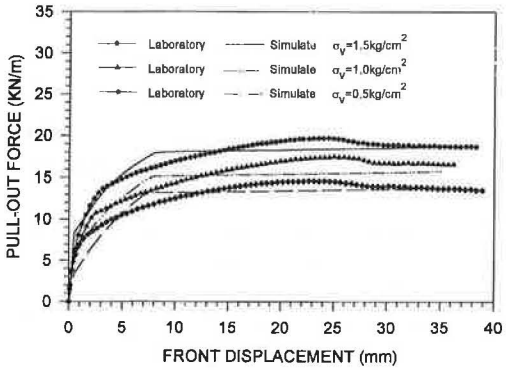

Figure 6--Pull-out force/displacement chart for laboratory test and numerical simulation of grid B confined under weathered mudstone.

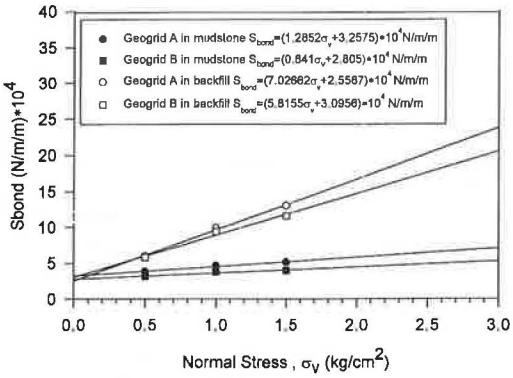

Figure 7--S_{bond}/Normal stress chart of geogrid confined by weathered mudstone and sandy-soil backfill.

Table 3: K_{bond} AND S_{bond} vaules selected for pull-out test

Geogrid A			Geogrid B	
K_{bond}	(N/m/m)	4.121×10^7	K_{bond} (N/m/m)	3.228×10^7
	σ_c=0.5 kg/cm²	3.846×10^4	σ_c=0.5 kg/cm²	3.159×10^4
	σ_c=1.0 kg/cm²	4.651×10^4	σ_c=1.0 kg/cm²	3.779×10^4
	σ_c=1.5 kg/cm²	5.131×10^4	σ_c=1.5 kg/cm²	4.000×10^4

integrate the foundation and the reinforcement materials, hence preventing their separation.

Analysis and Discussion of Laboratory Test Results

To better understand the frictional resistance of the geogrid and the interactive relationship of passive resistance in the pull-out test, this study removed the transverse ribs of the A and B grids to perform the pull-out test. By thus modifying the contact area of the geogrid, the frictional resistance of the entire grid can be calculated and can be compared to the pull-out resistance of the unmodified grid. Referencing the data in Figure 2 concerning the pull-out resistance of geogrids confined in sandy soils, frictional resistance comprises nearly 30 % of total pull-out resistance, and passive soil resistance makes up the remaining roughly 70 %. This data clearly demonstrates that passive soil resistance is much greater than frictional resistance. This same chart also shows that the pull-out resistance of geogrid A is higher than that of geogrid B. This is due to the thickness of A exceeding that of B by 1.2 mm; making the carrying capacity of A greater. From this it is evident that the carrying capacity of transverse ribs influences the utilization of passive resistance.

As is show in Figure 3, most of the pull-out resistance of the mudstone/geogrid is provided by frictional resistance. This figure also shows that for clayey soils, the function of frictional resistance is greater than that of passive resistance. Moreover, in the initial stage of pull-out--when displacement is less than 2 mm--total pull-out resistance is equal to frictional resistance. After pull-out exceeds 2 mm, pull-out resistance gradually becomes greater than frictional resistance. This phenomenon is due to the lack of relative displacement between soil and grid in the initial stage of pull-out, which stems from the elongation of the anterior portion of the geogrid specimen, and the main resistance to tension originating from the static friction between soil and geogrid. As for the passive soil mass, only partial plastic strain is produced, and failure of the soil mass does not occur. At this point, the soil and grid produce relative displacement. As the passive soil pressure of the anteirior transverse ribs is utilized, the total pull-out resistance gradually rises faster than frictional resistance. Figure 4 shows that under equivalent confining conditions, the pull-out resistance of geogrid A is greater than that of B. Most of the difference, however, is due to the disparity between the frictional resistance values of A and B. Therefore, although the thickness of the transverse ribs of grid A exceed that of B by 1.2 mm, there is still no significant difference in passive earth resistance. From this data, it can be determined that the pull-out resistance of the unidirectional geogrid and weathered mudstone, the passive earth pressure of the transverse ribs cannot be utilized. Therefore, frictional resistance comprises the most essential part of the tensional force.

Results and Discussion of Numerical Simulation Analysis

Based on the pull-out test results of weathered mudstone, the selected shear stiffness of grout (K_{bond}) and the slider cohesiveness of grout (S_{bond}) values are listed in Table 3. Using the FISH function of FLAC to calculate values, the numerical simulation pull-out test results are listed in Figures 5 and 6. These figures show that the total resistance of the numerical simulation were lower than results obtained from actual resistance testing. For pull-out stiffness, actual test results were conservative under low confining pressure, but overestimated actual condititions under high confining pressure. However, the S_{bond} for the normal stress function depends on the functional relationship of differing confinement stress (See Figure 7).

Figures 8 and 9 show results for stressed A and B geogrids respectively when confined under well-graded sand. For both grids, results are nearly identical, with the maximum force being 33 kN/m. However, due to uneven tension exerted on the grid, the posterior section of the grid did not undergo the

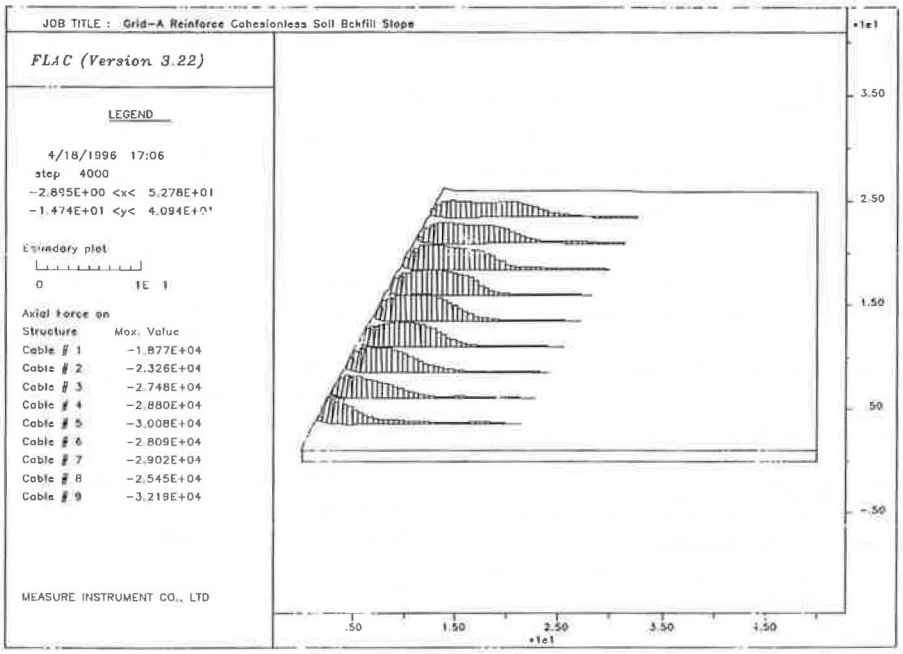

Figure 8--Chart of grid A reinforced slope, with well graded sand backfill, when subjected to force.

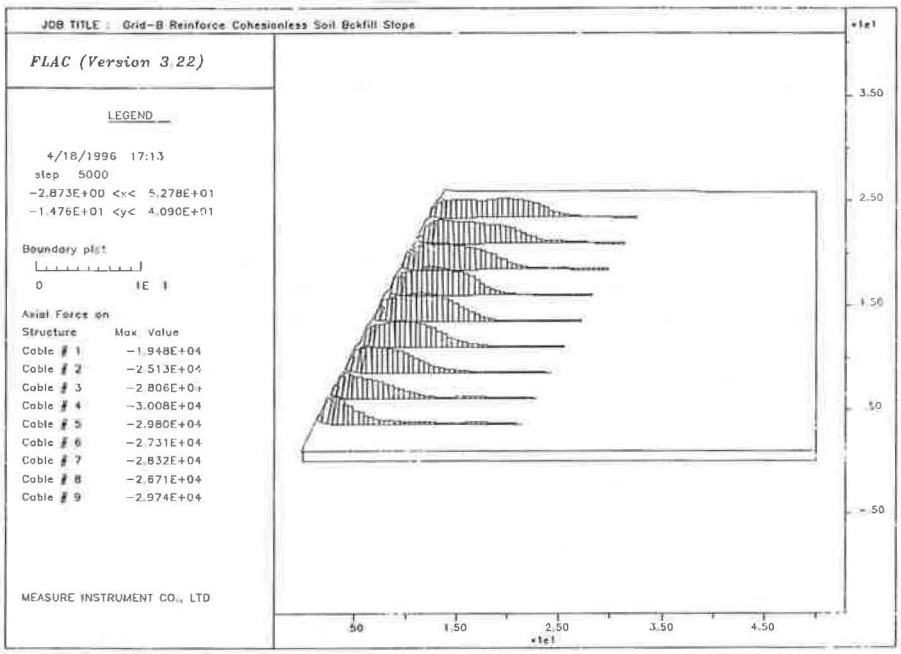

Figure 9--Chart of grid B reinforced slope, with wellgraded sand backfill, when subjected to force.

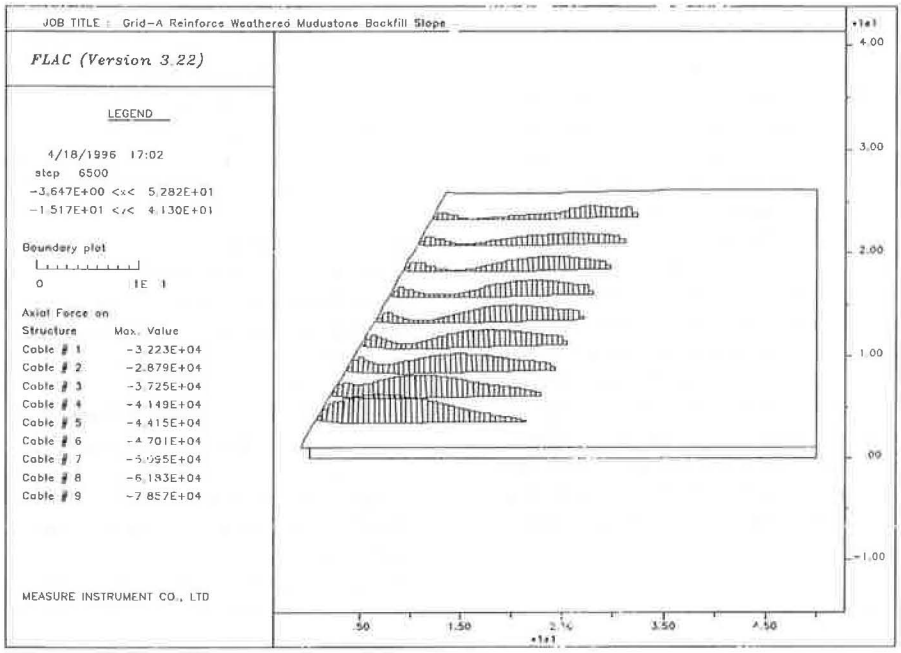

Figure 10--Chart of grid A reinforced slope, with weathered mudstone, when subjected to force.

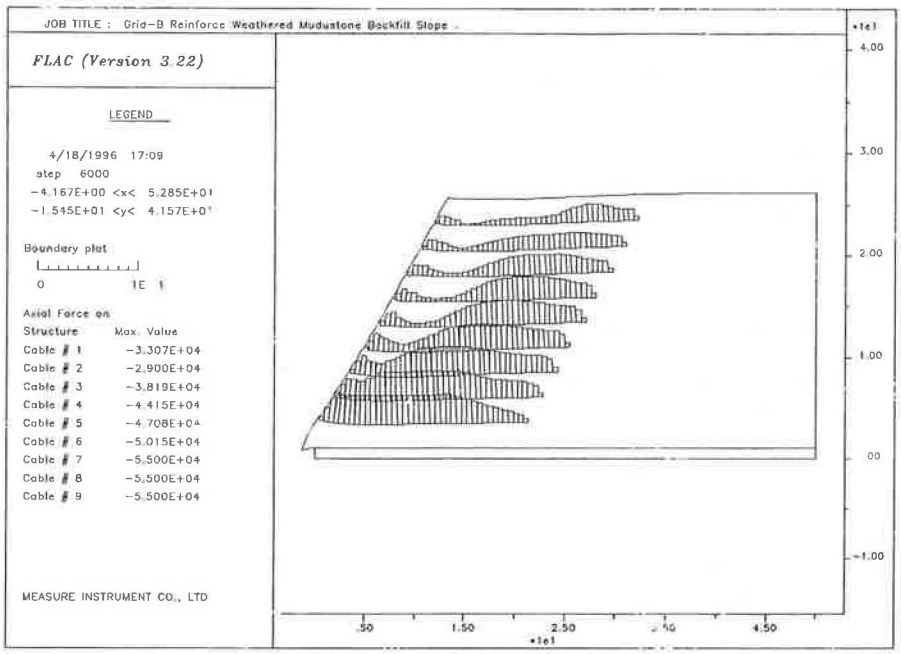

Figure 11--Chart of grid B reinforced slope with weathered mudstone, when subjected to force.

effects of stress. So, the over-extended portion remained buried. Figures 10 and 11 show the results for stressed A and B grids respectively when confined under weathered mudstone. Geogrid A approaches its maximum yeild at 80 kN/m. At this point, grid B has already failed. These figures also show that from the middle to the top layers, stress accumulates at the posterior section of the A and B grids. This is due to the influence of the soil's own weight, which gives the grid pull-out potential, and increases the stress of the posterior section.

Basically, the results of this study show that selection and installation of reinforcement material is critical. Pulling behaviors, safety considerations, and failure or near-failure conditions are extremely evident, and thus they become the motivation for constructing this model simulation. With these results, one can better understand rational design considerations such as anchorage and geogrid strength.

Conclusions and Suggestions

Based on the findings of this study, the following conclusions can be drawn and suggestions put forth regarding the mechanical properties of geogrids and the numerical analysis model:

1. When confined under granular soil, passive earth resistance is the main contributor to the pull-out resistance of the geogrid. For confinement under cohesive soils, the major portion of pull-out resistance is provided by frictional resistance.
2. In the initial stage (less that 2 mm or movement) of the test for pull-out resistance of a geogrid confined under cohesive soil, displacement originates from the elongation of the anterior section of the geogrid specimen. This is caused chiefly by the static friction provided by the pulling force between the soil and geogrid. When the soil and geogrid begin relative displacement, the passive earth pressure of the transverse ribs begins to be utilized.
3. Sand backfill material provides excellent reinforcing results. Due to a the low level of anchorage strength, using weathered mudstone as a confining material results in higher lateral pressure, which causes a great deal of deformation in the reinforcement structure and its possible failure. Therefore, designers seeking to solve this problem should use methods to increase anchorage strength. These critical installation results are provided to better illuminate design considerations.

References

1. Jewell, R.A., G.W.E. Milligan, R.W. Sarsby and D. Dubois. Interaction between Soil and Geogrids. *Proc. of the Symp. on Polymer Grid Reinforcement in Civil Eng.*, Thomas Telford Limited, London, U.K., 1984, pp.19-29.

2. Bauer, G.E., and Y.M. Mowafy. The Effect of Grid Geometry and Aggregate Size on the Stress Transfer Mechanism. *Proceedings of the 4th International Conference on Geotextiles, Geomembranes and Related Products*, Vol. 2, 1990, pp.801.
3. Ochiai, H., Hayashi, S. &Otani, J., Hirai, T. Evaluation of pull-out resistance of geogrid reinforced soils, *Proceedings of the International Symposium , on Earth Reinforcement Practice, Kyushu University, Fukuoka, Japan*, 1992, pp.141-146.
4. Koerner, R.M. *GRI Test Methods and Standards: Geogrid Pullout.* Geosynthetic Research Institute,Drexel University, Philadelphia, 1992.
5. Cundall, P. Fast Lagrangian Analysis of Continua, Version 3.2. ITASCA Consulting Group, INC. 1992.